Structure Factor and Elasticity of a Heat-Set Globular Protein Gel

Matthieu Pouzot, Taco Nicolai,* Dominique Durand, and Lazhar Benyahia

Polymères, Colloïdes, Interfaces, UMR CNRS, Université du Maine, 72085 Le Mans Cedex 9, France

Received August 1, 2003; Revised Manuscript Received November 21, 2003

ABSTRACT: Cross-correlation dynamic light scattering was used to measure the structure factor of heated solutions of the globular protein β-lactoglobulin at pH 7 and 0.1 M NaCl. After 24 h heating at 80 °C finite size aggregates are formed at protein concentrations below 15 g/L, whereas at higher concentrations turbid gels are formed. The gels may be considered as collections of randomly close packed "blobs" with a self-similar structure characterized by a fractal dimension $d_f = 2.0 \pm 0.1$. The concentration dependence of the structure factor was compared with that of the elastic shear modulus. The results for this particular protein system were consistent with predictions of the so-called fractal gel model. Limits of validity of the model are discussed.

Introduction

Heat-induced denaturation of globular proteins in aqueous solution often leads to irreversible aggregation, and gels may be formed above a critical concentration (C_g).[1] In general, for random cluster−cluster aggregation C_g decreases with the size of the system and becomes very small for macroscopic systems. However, for heated globular proteins the cluster growth stagnates as soon as all proteins have aggregated.[2] The implication is that the reactivity of the protein clusters is limited in time and that native proteins need to be present for the aggregation to continue. For $C < C_g$ all native proteins have aggregated, and the growth stagnates before the gel is formed.

The rate of gelation and the gel strength are strongly dependent on the temperature, the pH, the concentration, and the ionic strength. Far from the isoelectric point and at low ionic strength transparent gels are formed. Microscopy shows that linear aggregates are formed in these circumstances. At high ionic strength or close to the isoelectric point (pI) the gels are turbid and microscopy shows denser branched aggregates. C_g decreases with decreasing electrostatic interactions, i.e., at higher ionic strength or closer to the pI.

The structure factor of heat-set protein gels at small length scales has been studied using neutron and X-ray scattering.[3−5] They show for transparent gels a maximum caused by electrostatic interactions. Transparent gels are homogeneous at length scales larger than a few tens of nanometers and thus show no q dependence over the q range covered by light scattering. When the ionic strength is increased, the interaction peak disappears, and instead an increase of the scattering intensity is observed at low scattering wave vectors (q). So far structure factors of turbid gels could not be studied at the smaller q values covered by light scattering because multiple scattering influences the results. However, it has recently been shown that the structure factor of turbid globular protein gels can be determined using cross-correlation dynamic light scattering.[6]

The shear modulus of globular protein gels at given heating time increases strongly with increasing protein concentration. It was sometimes found that the elastic modulus (G_0) increased with C as $G_0 \propto C^n$ for C significantly larger than C_g.[3,7−11] Similar scaling of the shear modulus with the volume fraction has been observed for gels formed by aggregating spherical colloids.[12−16] These results have been interpreted in terms of the so-called fractal gel model. The basic assumption is that the colloidal gels can be modeled as a collection of close-packed connected "blobs" with molar mass M and size ξ. The blobs are formed by aggregates that grow until they fill up the space and connect to form the gel. The aggregates and thus the blobs have a self-similar internal structure that is characterized by a fractal dimension d_f, which implies that $M \propto \xi^{d_f}$. It follows that ξ decreases with increasing concentration as

$$\xi \propto C^{1/(d_f-3)} \tag{1}$$

Each blob acts as an elastic spring with an elastic constant K given by $K = K_0 N_b^{-1} \xi^{-2}$, where K_0 is the bending constant of the N_b links of the stress baring elastic backbone.[17] N_b is related to ξ through the fractal dimension of the elastic backbone, d_b, that is necessarily between unity and d_f : $N_b \propto \xi^{d_b}$. Since there are ξ^{-1} blobs per unit length, the elastic modulus of the system is given by

$$G_0 \propto \xi^{-(3+d_b)} \tag{2}$$

Consequently one obtains $G_0 \propto C^n$ with $n = (3 + d_b)/(3 - d_f)$. If the bending constant is small, we also have to consider the contribution of entropy to the elastic energy. In the limit of fully flexible blobs, i.e., $K_0 \to 0$, entropy dominates and the elastic energy per blob is approximately kT independent of ξ, with k Boltzmann's constant and T the absolute temperature. In this case one expects $G_0 \propto \xi^{-3}$.

This so-called fractal gel model has been applied to globular protein gels in the past, and values of the fractal dimension have been deduced from the concentration dependence of the shear modulus.[3,7−10] However, the validity of the basic assumptions of the model has so far not been tested for globular protein gels. This can be done by measuring both the structure factor and the shear modulus as a function of the concentration. If the sol fraction is negligible, the apparent molar mass (M_a) and radius of gyration (R_a) derived from the structure

* Corresponding author: e-mail Taco.Nicolai@univ-lemans.fr.

10.1021/ma035117x CCC: $27.50
Published on Web 12/25/2003

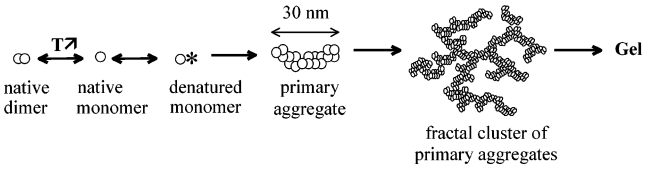

Figure 1. Schematic representation of the gel formation of heated β-lactoglobulin at pH 7 and 0.1 M salt.

factor are approximately equal to M and ξ. The aim of the present study is to test the validity of the fractal gel model for turbid globular protein gels by comparing the structure factor with the shear modulus.

The system we have investigated is β-lactoglobulin at pH 7 and 0.1 M NaCl. β-Lactoglobulin is a globular protein with molar mass 18.6 kg/mol and a radius of about 2 nm.[18,19] It is the main component of whey, and its heat-induced aggregation and gelation have been studied extensively in the past. The conditions of gelation were chosen such that electrostatic interactions are screened and fractal aggregates are formed in accordance with the assumptions of the model. The aggregation process under these conditions can be described schematically as follows (see Figure 1).[20,21] At room temperature the proteins are mainly present in the form of dimers. With increasing temperature the equilibrium shifts toward the monomeric form and the proteins denature. Denatured proteins associate to form small well-defined aggregates containing about 100 particles. These so-called preaggregates further associate to form large fractal clusters. The aggregation rate increases strongly with the temperature and more weakly with the protein concentration. The fractal dimension of the clusters is $d_f = 2$, and their structure is independent of the concentration and the heating temperature.

Materials and Methods

Materials. The β-lactoglobulin used in this study was a gift from Lactalis (Laval, France) and contained about equal fractions of the variants A and B. We showed elsewhere that the aggregation rate is equal for the two variants in the mixture.[22] Solutions were extensively dialyzed against salt-free Milli-Q water at pH 7 with 200 ppm of NaN_3 added to avoid bacterial growth. After the dialysis the ionic strength was set to 0.1 M with NaCl. For light scattering measurements the samples were filtered through 0.45 μm pore size Anotope filters. The concentration was measured after filtration by UV absorption at 278 nm using an extinction coefficient 0.96 L g^{-1} cm^{-1}.[23] Solutions in airtight light scattering cells were heated for 24 h in a thermostat bath at 80 °C and subsequently rapidly cooled to 20 °C. For shear measurements the samples were degassed and heated at 80 °C directly in the rheometer.

Light Scattering. Light scattering measurements were done at 20 °C using a commercial version of the 3D cross-correlation instrument described in ref 24 (LS Instruments, Fribourg, Switzerland). The light source was a diode laser with wavelength $\lambda = 685$ nm. Photon correlation was done with a digital correlator (ALV-5000E, ALV). The relative excess scattering intensity (I_r) was calculated as the intensity minus the solvent scattering divided by the scattering intensity of toluene at 20 °C. I_r was corrected for multiple scattering and the transmission as described in ref 6. Briefly, one measures the intercept of the intensity autocorrelation function, B, and uses the measured reduction of the intercept with respect to that of a transparent sample, B_0, to calculate the fraction of single scattered photons: $F_s = (B/B_0)^{0.5}$. Ideally $B_0 = 0.25$, but in the setup used here it was about 0.2 and depended slightly

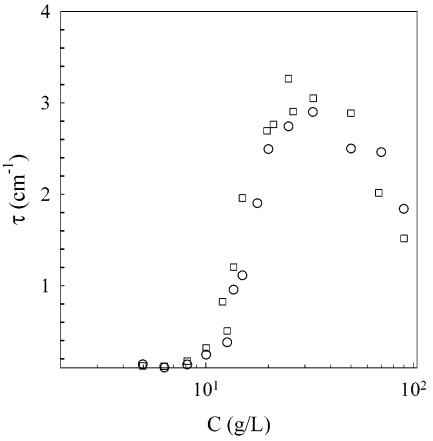

Figure 2. Concentration dependence of the measured turbidity (squares) of β-lactoglobulin solutions at pH 7 and 0.1 M NaCl after heating 24 h at 80 °C. The circles show the turbidity derived from light scattering results (see text).

on the scattering angle. The transmission, T_r, was calculated from the turbidity measured at the same wavelength, τ, and the path length of the light through the sample, L: $T_r = \exp(-\tau L)$. The single scattered light intensity is calculated as $I_r(\text{corr}) = [I_r(\text{exp})/T_r](B/B_0)^{0.5}$.

The terminal relaxation time of the autocorrelation function diverged close to the gel point, and gelled systems were nonergodic. To ensure full decay of the autocorrelation function and correct determination of the intercept, the samples were slowly rotated. I_r was measured as a function of the scattering wave vector (q) for each sample in light scattering cells with inner tube diameters of 4 mm. We measured the turbidity with a spectrometer at $\lambda = 685$ nm. By using cells with varying thickness between 10 and 1 mm, the turbidity could be determined with negligible effect of multiple scattering for the samples studied here.

In dilute solutions I_r is related to the weight-average molar mass (M_w) and the structure factor ($S(q)$) of the solute:[25,26]

$$I_r = HCM_wS(q) \tag{3}$$

with C the concentration and H an optical constant:

$$H = \frac{4\pi^2 n_s^2}{\lambda^4 N_a}\left(\frac{\partial n}{\partial C}\right)^2\left(\frac{n_{tol}}{n_s}\right)^2\frac{1}{R_{tol}} \tag{4}$$

Here N_a is Avogadro's number, $(\partial n/\partial C)$ is the refractive index increment, and R_{tol} is the Rayleigh constant of toluene at 20 °C. n_{tol} and n_s are the refractive indices of toluene and the solvent, respectively. $(n_{tol}/n_s)^2$ corrects for the difference in the scattering volume of the solution and the solvent. We have used $(\partial n/\partial C) = 0.189$ mL/g[27] and $R_{tol} = 1.02 \times 10^{-5}$ cm^{-1}.[28−30] $S(q)$ may be written in terms of the z-average radius of gyration (R_{gz}) of the solute if $qR_{gz} < 1$:

$$S(q) = (1 + q^2R_{gz}^2/3)^{-1} \tag{5}$$

At higher concentrations $S(q)$ is the structure factor of the solution, and M_w and R_{gz} should be replaced by an apparent molar mass (M_a) and radius (R_a).

It is obvious that the experimental error becomes important for samples that show strong multiple scattering and that are highly turbid. The error on the intercept B can be reduced by increasing the measuring time, and for the samples with the lowest intercepts (about 0.015) the measurements took several hours. In each case the intercept was measured at least twice. The error on $(B/B_0)^{0.5}$ was quite variable but never more than 20%. The experimental error on $S(q)$ is perhaps best judged from the scatter of the data shown in Figure 4b. There is uncertainty of about 10% in the horizontal and vertical shifts

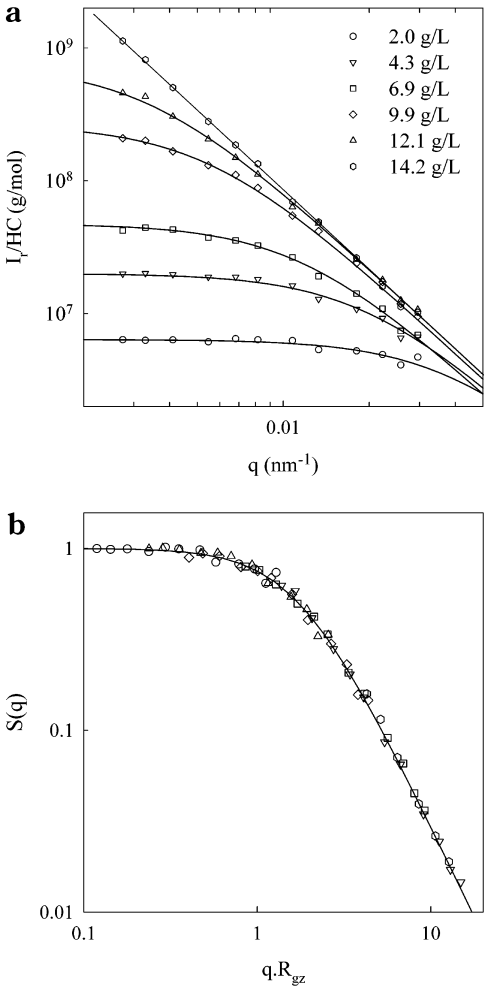

Figure 3. (a) Wave vector dependence of I_r/HC for highly diluted β-lactoglobulin aggregates formed after heating 24 h at 80 °C at different concentrations indicated in the figure (pH 7 and 0.1 M NaCl). The solid lines represent fits to the equation $I_r/HC = M_w(1 + q^2R_{gz}^2/3)^{-1}$. (b) Structure factor of highly diluted β-lactoglobulin aggregates formed after heating 24 h at 80 °C at different concentrations (pH 7 and 0.1 M NaCl). Symbols are as in (a). The solid line represents $S(q) = (1 + q^2R_{gz}^2/3)^{-1}$.

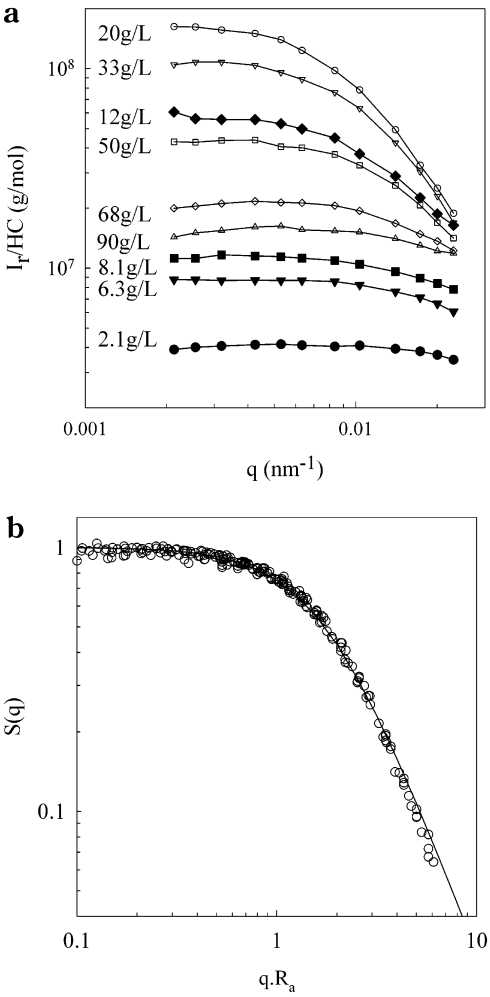

Figure 4. (a) Wave vector dependence of I_r/HC for β-lactoglobulin solutions at different concentrations indicated in the figure after heating 24 h at 80 °C (pH 7 and 0.1 M NaCl). Filled symbols represent data for $C < C_g$, and open symbols represent data for $C > C_g$. (b) Structure factor of β-lactoglobulin solutions at different concentrations after heating 24 h at 80 °C (pH 7 and 0.1 M NaCl). The solid line represents $S(q) = (1 + q^2R_a^2/3)^{-1}$.

used to obtain the mastercurves of $S(q)$ shown in Figures 3b and 4b. The turbidity was determined with an experimental error of about ± 0.2 cm^{-1}, which leads to an error of about 10% on T_r. The total experimental error on the determination of M_a and R_a is best judged from the scatter of the data in Figures 5 and 6. We expect that the systematic error due to the uncertainty of $(\partial n/\partial C)^2$ and R_{tol} is less than 10%.

Rheology. The shear modulus was measured at 0.1 Hz as a function of heating time with an ARES strain controlled rheometer. We used either a Couette (cup diameter 34 mm; bob diameter 32 mm) or a plate−plate (diameter 50 mm; gap 1 mm) geometry. The same results were obtained with both geometries, but the Couette geometry gives more reproducible results for the weaker gels formed close to C_g. The temperature was controlled at 80 °C with a Peltier system for the plate−plate geometry and with circulating water from a heat bath in the Couette geometry. The samples were covered with mineral oil to avoid evaporation. We checked that the mineral oil does not influence the aggregation process. A deformation of 5% was used which is still in the linear regime. We repeated the experiments at different deformations and found that the effect of strain was negligible up to a deformation of 10%. At higher strains the samples are first strain hardening until they break irreversibly above a critical value. Nonlinear rheological properties of the systems will be reported elsewhere.

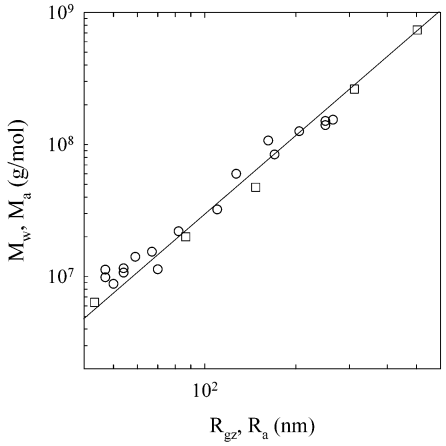

Figure 5. Comparison of the dependence of M_a on R_a (circles) with that of M_w on R_{gz} (squares). The solid line represents $M_a = 3 \times 10^3R_a^2$.

Results

Light Scattering. We investigated a series of β-lactoglobulin solutions at pH 7 and 0.1 M NaCl that were

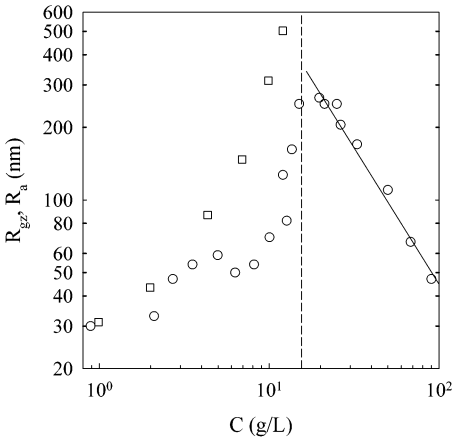

Figure 6. Comparison of the concentration dependence of R_a (circles) and R_{gz} (squares). The dashed line indicates the gel concentration, C_g, and the solid line has slope −1.1.

heated at 80 °C for 24 h. We found with size exclusion chromatography that the fraction of unaggregated protein is 5% over the whole range of concentrations investigated. Figure 2 shows that the turbidity of the heated solutions increases up to $C \approx 30$ g/L and decreases at higher concentrations. For $C < C_g = 15$ g/L the solutions do not gel, and we can characterize the aggregates in dilute solutions where interaction between the aggregates is negligible. Figure 3a shows the q dependence of $I_r/(HC)$ of very dilute aggregates obtained at different concentrations below C_g. The structure factor of the aggregates is plotted in Figure 3b as a function of qR_{gz}. It can be well described by eq 5 over the whole range of qR_{gz}.

Figure 4a shows the q dependence of $I_r/(HC)$ at different concentrations for undiluted systems. The structure factor of the samples is plotted in Figure 4b as a function of qR_a. The solid line through the data represents again eq 5 (replacing R_{gz} by R_a) and shows that the structure factor of the undiluted systems is almost the same as that of the diluted aggregates. The shape of structure factor depends on the size distribution and the form factor of the aggregates or the blobs. Therefore, one should not expect the structure factors to be exactly the same even if the internal structure is identical. In Figure 5, we compare the dependence of M_a on R_a for the blobs with the dependence of M_w on R_{gz} for the diluted aggregates. Within the experimental error the dependences are the same which is consistent with the observation that the structure factors are the same. We note that the value of M_a is sensitive to the precise value of the turbidity and is therefore less certain for the more turbid samples. The solid line in Figure 5 has slope 2, implying that $d_f = 2$.

The concentration dependence of R_a and R_{gz} is shown in Figure 6. For very dilute solutions interactions between the aggregates are small and $R_a \approx R_{gz}$. With increasing concentration the aggregates become bigger and R_{gz} diverges at C_g. However, R_a remains finite due to excluded-volume interaction that increases with increasing concentration. Above $C \approx 20$ g/L interaction dominates, and R_a decreases approximately linearly with C: $R_a \propto C^{-1.1}$ (see the solid line in Figure 6).

The turbidity can be calculated from the q-dependent light scattering results:

$$\tau = H'CM_a \int_0^{2\pi} \int_0^{\pi} S(q)(1 + \cos^2\theta) \sin\theta \, d\theta \, d\varphi \quad (6)$$

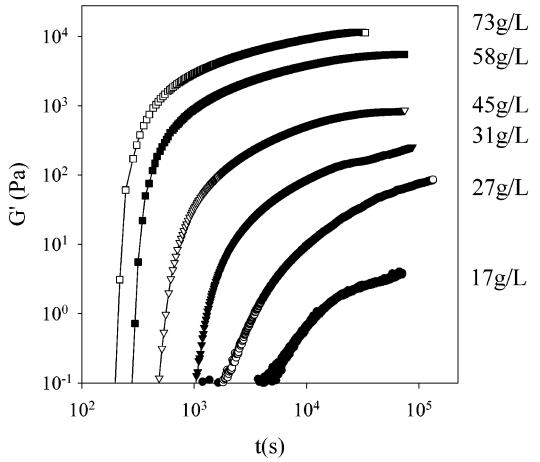

Figure 7. Evolution of the storage shear modulus at 0.1 Hz with heating time at 80 °C for β-lactoglobulin solutions at different concentrations indicated in the figure (pH 7 and 0.1 M NaCl).

where $H' = HR_{tol}(n_s/n_{tol})^2$. Using $S(q) = (1 + q^2R_a^2/3)^{-1}$, the integral can be solved analytically:

$$\tau = H'CM_a 2\pi \left[\frac{-4}{a^2}(a + 2) + \frac{8a + 4a^2 + 8}{a^3} \ln(1 + a) \right] \quad (7)$$

with

$$a = \left(\frac{4\pi n}{\lambda} \frac{R_a}{\sqrt{3}} \right)^2$$

We have calculated the turbidity as a function of C using the values of R_a shown in Figure 6 and using the experimental power law relation $M_a = 3 \times 10^3 R_a^2$ shown in Figure 5. The calculated values are compared to the measured values in Figure 2. The results of the two techniques are consistent within the experimental error.

Shear Modulus. Figure 7 shows the evolution of the storage shear modulus (G') at 0.1 Hz for different protein concentrations at 80 °C. Above the gel time (t_g) G' increases rapidly at first and later continues to increase slowly over the whole duration of the measurement. The gel time increases with decreasing concentration and diverges as $C \to C_g$. We will report a detailed account of the shear measurements including the temperature and frequency dependence elsewhere. All we need to know here is that after 24 h at 80 °C we find that G' is almost independent of the frequency in the range 0.01−10 Hz and that $G' \gg G''$. This means that we may equate G' at 0.1 Hz with the elastic modulus G_0.

The concentration dependence of G' after 24 h heating is shown in Figure 8. For $C > 20$ g/L the concentration dependence can be approximated by a power law dependence: $G' \propto C^{4.5}$ (see the solid line in Figure 8). At lower concentrations G' decreases strongly, and for $C \leq 15$ g/L the system does not gel in a period of 24 h. Renard et al.[3] measured the concentration dependence of G' for β-lactoglobulin after heating at 80 °C for 1 h under the same conditions. They observed a stronger concentration dependence ($G' \propto C^{6.1}$) in the range 25−60 g/L covered in their experiment. Verheul and Roefs[7] found $G' \propto C^{4.5}$ in the range 35−80 g/L for a whey protein isolate containing 70% β-lactoglobulin after heating at 68.5 °C for 20 h under the same conditions.

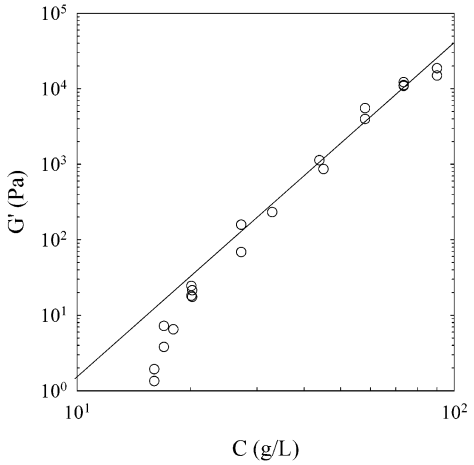

Figure 8. Concentration dependence of the storage shear modulus at 0.1 Hz of β-lactoglobulin solutions after heating 24 h at 80 °C (pH 7 and 0.1 M NaCl). The solid line has slope 4.5.

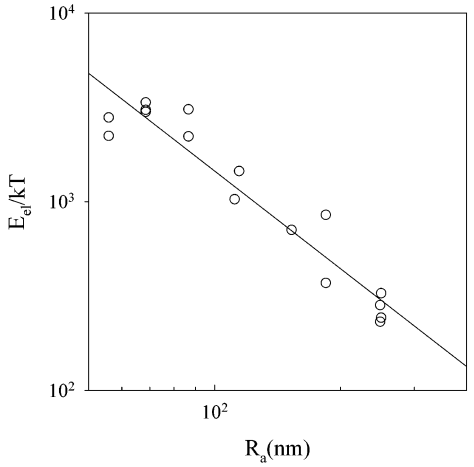

Figure 9. Normalized elastic energy of β-lactoglobulin solutions after heating 24 h at 80 °C as a function of R_a for $C > 20$ g/L (pH 7 and 0.1 M NaCl). The solid line has slope −1.5.

Obviously, the concentration dependence of G' depends on the heating time (and temperature), because G' evolves differently at different concentrations especially close to C_g. Therefore, one should be cautious when comparing data obtained with different heat treatments. For example, we also found a stronger concentration dependence of G' after heating for 1 h at 80 °C. After cooling to 20 °C the gel modulus increases by a factor of 2−3 independent of the concentration similar to that reported by Renard et al.[3]

Discussion

After 24 h heating at 80 °C practically all proteins have aggregated to form aggregates with an average size that increases with increasing protein concentration. At low concentrations the aggregates are small and still dilute so that $R_a \approx R_{gz}$. R_a increases less rapidly than R_{gz} with increasing protein concentration due to excluded-volume interaction between the aggregates. The concentration, C^*, at which the aggregates occupy the whole volume can be estimated from

$$C^* = \frac{3M_w}{N_a 4\pi {R_{gz}}^3} \tag{8}$$

Using the experimentally observed dependence of M_w and R_{gz} on C, we find $C^* \approx 7$ g/L. But notice that this value is only a rough estimate because we ignored the effect of polydispersity. At higher concentrations the aggregates are strongly interpenetrated so that R_a no longer depends on R_{gz}. The system may be described as a collection of randomly close-packed blobs with radius R_a and molar mass M_a if $R_a \propto C^{1/(d_f-3)}$ and $M_a \propto {R_a}^{d_f}$. These relations are consistent with the experimental results for $C > 20$ g/L with $d_f = 2.0 \pm 0.1$.

The same approach was used to explain successfully the concentration dependence of R_a in gels formed by randomly aggregating charged silica particles.[31] Also for that system the structure factor could be fitted to eq 5 for small qR_a, but a slightly stronger power law dependence was found for large qR_a. In a different system of randomly aggregating charged disklike mineral particles similar structure factors were observed,[32] but for this system R_a was found to be strongly dependent on the ionic strength, indicating the influence of long-range electrostatic interactions. For these systems, as for heated globular proteins, the aggregation process is reaction controlled and therefore relatively slow.

When repulsive interactions are fully absent, the aggregation becomes diffusion-controlled. Diffusion-controlled cluster aggregation (DLCA) leads to rather monodisperse size distributions, and the clusters develop a depletion layer. As a consequence, the structure factor shows a peak at $q \approx \pi/R_a$.[33,34] Reaction-controlled cluster aggregation (RLCA) leads to rather polydisperse size distributions, and there is no depletion layer so that such peaks are not observed. However, even though $S(q)$ is very different, the argument that leads to the power law relation $R_a \propto C^{1/(d_f-3)}$ is valid for both DLCA and RLCA as long as there are no long-range interactions between the particles.[34]

Of course, one should not take the image of blobs literally. R_a simply corresponds to the correlation length of protein concentration fluctuations. On average, the concentration at distance r from any given protein decreases as $C \propto r^{d_f-3}$ until at $r \approx R_a$ it is equal to the average concentration. This is obvious from the observation that the blob size increases if we progressively dilute solutions below the gel point.[6] It is clear that it makes no sense to literally distinguish bonds inside the blobs and between blobs.

It is important to realize that the fractal gel model discussed in the Introduction is only valid if the sol fraction is negligible, i.e., not close to C_g. The sol fraction does not contribute to the elastic modulus, although it does contribute to the shear modulus at higher frequencies. Only if the sol fraction is negligible is the size of the structural units of the gel (ξ) directly proportional to R_a determined with light scattering. In this study we have shown that the concentration dependence of the blob size obtained from light scattering is consistent with that of the gel modulus for C not close to C_g, i.e., when the sol fraction is negligible. This comparison represents the first direct verification of the fractal gel model.

Another assumption of the fractal gel model is that the origin of the elasticity is enthalpic. We have calculated the elastic energy per blob as $E_{el} = 3G'/(4\pi {R_a}^3)$. Figure 9 shows E_{el} normalized by the thermal energy (kT) as a function of R_a for $C > 20$ g/L. E_{el}/kT is equal to the elastic modulus normalized by the osmotic modulus. If the elastic energy is dominated by entropy,

we expect that $E_{el} \approx kT$, while if the bending energy dominates we expect that $E_{el} \gg kT$ and that $E_{el} \propto R_a^{-d_b}$. Clearly the bending energy dominates at least for $C >$ 20 g/L. The straight line through the data has a slope of −1.5, implying that $d_b \approx 1.5$. However, this calculation is based on data obtained after 24 h, and we have ignored the time dependence of G'. This means that the true value of d_b is somewhat smaller. At 20 °C the elastic modulus is larger, but the concentration dependence is about the same. The temperature dependence of the elastic modulus is probably caused by a temperature dependence of the bending constant of the individual bonds.

We will now discuss the deviation from the power law concentration dependence of G_0 close to C_g. For the present system (pH 7 and 0.1 M NaCl) we find that the sol−gel transition occurs approximately at $C_g = 15$ g/L. Light scattering shows that at this concentration the aggregates are already strongly interpenetrated. We may therefore describe the sol−gel transition as a bond percolation process of close packed blobs. Whereas light scattering is sensitive to the structure of the whole system, the elastic modulus is determined by the structure of the gel. If the gel fraction (F_g) is less than unity, the size of the structural unit of the gel is larger than R_a. We would measure ξ with light scattering if we could remove the very polydisperse sol fraction. However, we cannot probe with light scattering the structure of the gel on length scales larger than R_a as it is screened by the sol fraction.

At the gel point, F_g is almost zero and ξ is equal to the sample size. Just above the gel point, the gel fraction increases and ξ decreases rapidly with an increasing number of junctions (n) between the blobs while R_a remains almost constant. The percolation model[35] predicts that ξ and F_g have a power law dependence on $\epsilon = (n - n_c)/n_c$ for $\epsilon \ll 1$, with n_c the number of links at the gel point: $\xi \propto \epsilon^{-0.88}$ and $F_g \propto \epsilon^{0.41}$. n increases with increasing heating time at a fixed concentration and with increasing protein concentration at a fixed heating time. Percolation of blobs would explain the initial rapid increase of the modulus above t_g. The subsequent slow increase could be a consequence of a slow increase of n or it could be caused by a slow increase of K_0. In addition, at higher protein concentrations a sizable fraction of proteins has not yet aggregated at t_g and could reinforce the gel structure after the gel has been formed.[2,36] However, after 24 h heating almost all the native proteins have aggregated. This means that except close to C_g the sol fraction after 24 h heating is negligible and ξ may be equated with R_a.

In the previous discussion it was assumed that the shear modulus at 0.1 Hz represents the elastic modulus. As mentioned above, we have verified that this is indeed the case for the data presented here. However, we did observe a strong increase of the shear modulus at higher frequencies for systems that are close to the gel point. This frequency dependence is caused by the relaxation of the sol and the gel on length scales smaller than ξ. At the gel point one might expect that the frequency dependence extents to very low frequencies. Unfortunately, the shear modulus of the systems at and below the gel point is very small ($G' < 0.01$ Pa) and cannot be determined with the equipment used here.

In conclusion, the particular heat-set protein gels that we studied here can be successfully described as ensembles of close packed fractal blobs with an elastic energy dominated by their bending energy. However, the validity of this description is subject to a number of conditions. (1) The concentration and heating times need to be sufficiently high so that the sol fraction can be ignored; otherwise $\xi > R_a$. (2) R_a needs to be larger than the elementary unit of the fractal structure, which may itself be significantly larger than the individual proteins. Small-angle neutron scattering measurements showed that for the system studied here the elementary unit, i.e., the primary aggregate, has a radius of about 15 nm.[16] How much larger R_a needs to be has to be established experimentally. (3) The interaction between the proteins should be short-range and repulsive since long-range electrostatic interaction decreases R_a as was observed for charged colloid gels. In addition, if electrostatic interactions are important, generally heated globular proteins form linear aggregates that are only weakly branched. On the other hand, attractive interactions may lead to the formation of heterogeneous gels containing dense microdomains if the aggregates have some flexibility and can rearrange. This is the case for gels formed by heated globular proteins close to the isoelectric point or at very high ionic strength.

Therefore, we expect that the fractal gel model is valid for heat-set protein gels only over a limited range of concentrations at a pH that is close, but not too close, to pI or at a ionic strength that is high, but not too high. We are currently investigating the limits of the validity of the fractal gel model for heat-set protein gels by studying the influence of electrostatic interactions on the structure and the elastic modulus.

Acknowledgment. We thank Unilever at Colworth (U.K.) for financial support and Allan Clark for fruitful discussions.

References and Notes

(1) Clark, A. H. In *Functional Properties of Food Macromolecules*; Mitchell, J. R., Ed.; Elsevier Applied Science: London, 1998; p 77.
(2) Le Bon, C.; Nicolai, T.; Durand, D. *Macromolecules* **1999**, *32*, 6120.
(3) Renard, D.; Axelos, A.; Lefebvre, J. In *Food Macromolecules and Colloids*; Dickenson, E., Lorient, D., Eds.; Royal Society of Chemistry: Cambridge, 1995; p 390.
(4) Clark, A. H.; Tuffnell, C. D. *Int. J. Peptide Res.* **1980**, *16*, 339.
(5) Weyers, M.; Visscher, R. W., Nicolai, T.; Pouzot, M. Unpublished results.
(6) Nicolai, T.; Urban, C.; Schurtenberger, P. *J. Colloid Interface Sci.* **2001**, *240*, 419.
(7) Verheul, M.; Roefs, S. P. F. M. *Food Hydrocolloids* **1998**, *12*, 17.
(8) Ikeda, S.; Foegeding, E. A.; Hagiwara, T. *Langmuir* **1999**, *15*, 8584.
(9) Hagiwara, T.; Kumagai, H.; Matsunaga, T.; Nakamura, K. *Biosci. Biotechnol. Biochem.* **1997**, *61*, 1663.
(10) Vreeker, R.; Hoekstra, L. L.; den Boer, D. C.; Agterof, W. G. M. *Food Hydrocolloids* **1992**, 6, 423.
(11) Puyol, P.; Pérez, M. D.; Horne, D. S. *Food Hydrocolloids* **2001**, *15*, 233.
(12) Shih, W.; Shih, W. Y.; Kim, S.; Liu, J.; Aksay, I. A. *Phys. Rev. A* **1990**, *42*, 4772.
(13) Gisler, T.; Ball, R. C.; Weitz, D. A. *Phys. Rev. Lett.* **1999**, *82*, 1064.
(14) Rooij, R.; van der Ende, D.; Duits, M. H. G.; Mellema, J. *Phys. Rev. E* **1994**, *49*, 3038.
(15) Buscall, R.; Mills, P. D. A.; Goodwin, J. W.; Lawson, D. W. *J. Chem. Soc., Faraday Trans. 1* **1988**, *84*, 4249.
(16) Mellema, M.; van Opheusden, J. H. J.; van Vliet, T. *J. Rheol.* **2002**, *46*, 11.
(17) Kantor, Y.; Webman, I. *Phys. Rev. Lett.* **1984**, *52*, 1891.

(18) Papiz, M. Z.; Sawyer, L.; Eliopoulos, E. E.; North, A. C. T.; Findlay, J. B. C.; Sivaprasadarao, R.; Jones, T. A.; Newcomer, M. E.; Kraulis, P. J. *Nature (London)* **1986**, *324*, 383.
(19) Pessen, H.; Kumosinski, T. F.; Farrell, H. M. J. *J. Ind. Microbiol.* **1988**, *3*, 89.
(20) Aymard, P.; Gimel, J. C.; Nicolai, T.; Durand, D. *J. Chim. Phys.* **1996**, *93*, 987.
(21) Le Bon, C.; Nicolai, T.; Durand, D. *Int. J. Food Sci. Technol.* **1999**, *34*, 451.
(22) Le Bon, C.; Durand, D.; Nicolai, T. *Int. Dairy J.* **2002**, *12*, 671.
(23) Townend, R.; Winterbottom, R. J.; Timasheff, S. N. *J. Am. Chem. Soc.* **1960**, *82*, 3161.
(24) Urban, C.; Schurtenberger, P. *J. Colloid Interface Sci.* **1998**, *207*, 150.
(25) Brown, W., Ed. *Light Scattering. Principles and Developments*; Clarendon Press: Oxford, 1996.
(26) Higgins, J. S.; Benoit, H. C. *Polymers and Neutron Scattering*; Clarendon Press: Oxford, 1994.
(27) Perlmann, G. E.; Longsworth, L. G. *J. Am. Chem. Soc.* **1948**, *70*, 2719.
(28) Moreels, E.; De Ceunink, W.; Finsy, R. *J. Chem. Phys.* **1987**, *86*, 618.
(29) Bender, T. M.; Lewis, R. J.; Percora, R. *Macromolecules* **1986**, *19*, 244.
(30) Finnigan, J. A.; Jacobs, D. J.*Chem. Phys. Lett.* **1970**, *6*, 141.
(31) Dietler, G.; Aubert, C.; Cannel, D. S.; Wiltzius, P. *Phys. Rev. Lett.* **1986** *57*, 3117.
(32) Nicolai, T.; Cocard, S. *Eur. Phys. J. E* **2001**, *5*, 221.
(33) Carpinetti, M.; Giglio, M. *Phys. Rev. Lett.* **1993**, *70*, 3828.
(34) Bibette, J.; Mason, T. G.; Gang, H.; Weitz, D. A. *Phys. Rev. Lett.* **1992**, *69*, 981.
(35) Stauffer, D.; Aharony, A. *Percolation Theory*, 2nd ed.; Taylor & Francis: London, 1992.
(36) Verheul, M.; Roefs, S. P. F. M. *J. Agric. Food Chem.* **1998**, *46*, 4909.

MA035117X